

RSC Advances



This is an *Accepted Manuscript*, which has been through the Royal Society of Chemistry peer review process and has been accepted for publication.

Accepted Manuscripts are published online shortly after acceptance, before technical editing, formatting and proof reading. Using this free service, authors can make their results available to the community, in citable form, before we publish the edited article. This *Accepted Manuscript* will be replaced by the edited, formatted and paginated article as soon as this is available.

You can find more information about *Accepted Manuscripts* in the [Information for Authors](#).

Please note that technical editing may introduce minor changes to the text and/or graphics, which may alter content. The journal's standard [Terms & Conditions](#) and the [Ethical guidelines](#) still apply. In no event shall the Royal Society of Chemistry be held responsible for any errors or omissions in this *Accepted Manuscript* or any consequences arising from the use of any information it contains.

Interfacial properties and thermo-oxidative stability of carbon fiber reinforced methylphenylsilicone resin composites modified with polyhedral oligomeric silsesquioxanes in the interphase

Guangshun Wu,^a Lichun Ma,^a Yuwei Wang,^{ab} Li Liu,^{*a} and Yudong Huang^a

^a School of Chemical Engineering and Technology, Harbin Institute of Technology, Harbin 150001, China

^b College of Materials Science and Engineering, Qiqihar University, Qiqihar 161006, China

Abstract: The grafting of TriSilanolPhenyl-polyhedral oligomeric silsesquioxanes (TriSilanolPhenyl-POSS) onto the carbon fibers (CFs) was achieved via toluene-2,4-diisocyanate (TDI) as the bridging agent. Fourier transform infrared spectroscopy (FTIR) and X-ray photoelectron spectroscopy (XPS) confirmed the successful modification of TriSilanolPhenyl-POSS. Scanning electron microscopy (SEM) and atomic force microscopy (AFM) images showed that TriSilanolPhenyl-POSS nanoparticles were grafted uniformly onto the surface of CFs and the surface roughness increased significantly. The results of dynamic contact angle (DCA) demonstrated an improvement in the surface energy and wettability that related to the increased polarity of the obtained hybrid fibers (CF-g-POSS). The effects of TriSilanolPhenyl-POSS grafting on interfacial, impact, and heat-resistant properties of methylphenylsilicone resin (MPSR) composites were also studied. The interlaminar shear strength (ILSS) and impact resistance of methylphenylsilicone resin (MPSR)

composites after POSS modification were improved significantly with increasing amplitude of 41.91% and 28.65%, respectively. Moreover, the interfacial reinforcing and toughening mechanisms of composites have also been discussed. In addition, the thermal oxygen aging experiments indicated a remarkable improvement in the heat oxidation resistance by the introduction of TriSilanolPhenyl-POSS in the interphase. Meanwhile, the grafting processes do not decrease fiber tensile strength (TS).

1. Introduction

Methylphenylsilicone resin (MPSR) has been used widely not only as high performance structural materials but also as heat resistant applications in aerospace, marine and automobile industries owing to superior thermal-oxidative resistance and weather aging resistance.^{1,2} The superior mechanical, electrical and thermal properties and good biocompatibility of carbon fibers (CFs) make them ideal reinforcements for fabricating advanced polymer matrix composites.³⁻⁷ The performance of CFs reinforced polymer composites depends strongly on the quality of fiber-matrix interphase.⁸ An optimum interphase is required for the resulting composites to transfer the mechanical stress efficiently from matrix resin to the reinforcements, which contributes to relieve stress concentrations and enhance mechanical properties.^{9,10} However, applications of CFs/MPSR composites are restricted owing to the poor interfacial adhesion between the fibers and matrix resin. To ensure that CFs/MPSR composites can be used safely under complicated environmental conditions and to exploit the outstanding heat oxidation resistance more effectively, a sufficient and appropriate interfacial adhesion is of crucial importance. And the interfacial strength is dependent highly on interfacial structure and

molecular interaction.¹¹ But the non-polar, smooth and inert graphitic surface of CFs could result in lack of interfacial chemical bonds and effective physical interactions without fiber surface modification.^{12,13} As a result, various surface treatments methods, like oxidation treatments,^{14,15} chemical grafting,^{16,17} polymer sizing,^{18,19} high energy irradiation,²⁰ have been developed to activate fiber surface, change the surface wettability, improve surface roughness or form interfacial bonding between CFs and matrix resin.

Functional nanofillers, such as carbon nanotubes,^{21,22} graphene oxide,^{23,24} nanoclay,²⁵ carbon nanofibers,²⁶ silica nanoparticles²⁷ and iron oxide nanoparticles,²⁸ are considered as attractive reinforcements in advanced nanocomposite fields owing to their unique structures, nanoscale size, low density and superior properties. These functional nanofillers serving as novel coupling agents are beneficial to enhance interfacial polymer-filler interaction, and thus improve mechanical, electrical, thermal and magnetic properties of polymer nanocomposites. Noteworthy, Polyhedral oligomeric silsesquioxanes (POSS) has attracted great scientific interest from many research groups working in the area of high-performance polymer composites.²⁹ POSS is a type of organic-inorganic hybrids, which possesses an inner inorganic silicon-oxygen framework with a 0.53 nm side length and external eight organic substituents surrounding the cage-like core structure.³⁰⁻³² The external organic groups not only make POSS more compatible with the hot matrix resin but also provide the reactive sites for further functionality. POSS nanoparticles have attracted considerable attention as ideal reinforcing fillers for polymer composites. The introduction of POSS molecules can

improve the mechanic properties and thermal stability of polymer composites obviously.^{33,34} Our previous researches have demonstrated the ability of POSS grafted onto the surface of CFs to improve the interfacial properties of composites greatly by improving wettability, enhancing surface roughness to produce better mechanical interlocking and creating chemical bonding between CFs and the matrix resin.³⁵⁻³⁸ However, to the best of our knowledge, surface treatment of CFs with TriSilanolPhenyl-POSS has not been reported yet. Toluene-2,4-diisocyanate (TDI) with two different active isocyanate groups is utilized to establish the bridging agent. TriSilanolPhenyl-POSS is a type of POSS of the open-cage-like structure with an inorganic silsequioxane at the core, organic phenyl groups attached at the corners of the cage and three silanol (Si-OH) groups. The active silanols are unique given the proclivity of most Si-OH groups to eliminate water and form siloxane (Si-O-Si) linkages. The three active silanols of TriSilanolPhenyl-POSS not only can be grafted onto the fiber surface by one silanol but also form chemical bonding with silanol end groups of MPSR to improve the interfacial performance during the preparation processes. Therefore, the objective of this study is to graft TriSilanolPhenyl-POSS onto the fiber surface to improve the interfacial properties of CFs/MPSR composites. Moreover, the heat-resistant behaviors of MPSR composites were studied systematically.

In the present work, TriSilanolPhenyl-POSS was grafted onto the surface of CFs to improve the interfacial properties of composites using TDI as the bridging agent. After TriSilanolPhenyl-POSS modification, the surface roughness and wettability of CFs

were improved. The interphase consisting of TriSilanolPhenyl-POSS can increase significantly heat oxidation resistance of composites based on strengthened interfacial adhesion as well as superior thermal stability of TriSilanolPhenyl-POSS. The surface chemical composition of CFs before and after modification was testified by XPS. The surface topographies of the different CFs were observed by SEM and AFM. The wettability and surface free energy of untreated and modified CFs were studied by DCA. The effects of TriSilanolPhenyl-POSS grafting on the interfacial performance, impact toughness and heat resistance of CFs/MPSR composites were investigated by ILSS, impact tests and thermal oxygen aging experiments, respectively. The fractured surface morphologies of CFs/MPSR composites were studied by SEM.

2. Materials and methods

2.1 Materials

CFs, with an average diameter of 7 μm , were obtained from Toray Industries, Inc. TriSilanolPhenyl-POSS was purchased from Hybrid Plastics Co., Inc. Hydroxyl-terminated MPSR was obtained from ShangHai Chemicals Co. Toluene-2, 4-di-isocyanate (TDI), dibutyltindilaurate and Lithium Aluminium Hydride (LiAlH_4) were received from TCI Ltd. Toluene, concentrated nitric acid and tetrahydrofuran were supplied by Tianjin Bodi Organic Chemicals Co. Ltd and were reagent-grade. Toluene was distilled for purification prior to use. The molecular structure of TriSilanolPhenyl-POSS is shown in Fig. 1.

Insert Fig. 1 here

2.2 Surface functionalization of POSS onto CFs

POSS grafted CF was fabricated by several steps of chemical reactions. Firstly, the CFs were refluxed in acetone solution for 24 h to remove pollutants and polymer sizing (denoted as untreated CF). Secondly, the CFs were oxidized in concentrated HNO₃ at 80 °C for 4h and washed with deionized water until the pH value reached 7 and then dried. The oxidize fibers were then reduced in LiAlH₄-THF saturated solution, and allowed to react under reflux for 2 h. The obtained fiber provides the reactive sites of homogeneously hydroxyl groups for further functionality with TDI. After being washed with ethanol and dried, the CFs, excess TDI and 2-3 drops dibutyltin dilaurate were added in anhydrous toluene solution (100 mL) and react at 60 °C under stirring for 8 h to obtain TDI functionalized carbon fibers (denoted as CF-TDI). Finally, CF-TDI was reacted with TriSilanolPhenyl-POSS (0.5 g) in anhydrous toluene (100 mL) by mechanical agitation at 60 °C for 24 h. The modified fiber (CF-g-POSS) was washed by excel toluene under sonication to remove unreacted and physical-absorbed POSS. All the reactions were performed under the protection of N₂ atmosphere. The whole functionalization processes of preparing CF-g-POSS are illustrated in Fig. 2.

Insert Fig. 2 here

2.3 Fabrication of CFs/MPSR composites

CFs/MPSR composites were prepared by the compression molding method. Briefly, the unidirectional prepreg of CFs and MPSR was casted into a mold, and the preparation of composites was at 120 °C and 150 °C for 1 h without pressure, 180 °C under 20 MPa for 2 h and 250 °C under 20 MPa for 4h. When the curing process had finished, the mold was cooled to room temperature with the pressure being maintained. The fiber content

of composites was controlled in the range of 60-70 mass%, and the specimens were 6 mm in width and 2 mm in thickness.

2.4 Characterization techniques

The surface functional groups of CFs were analyzed by FTIR spectrophotometer (Nicolet, Nexus670, USA) using powder-pressed KBr pellets. The FTIR spectra were acquired by scanning the specimens for 64 times in the wavenumber range of 400-4000 cm^{-1} with the resolution of 2 cm^{-1} .

XPS (ESCALAB 220i-XL, VG, UK) was performed to detect surface composition and elucidate the grafting reaction procedures using a monochromatic Al Ka source (1486.6 eV) at a base pressure of 2×10^{-9} mbar. The XPS peak version 4.1 program was used for data analysis.

The surface morphologies and roughness (Ra) of CFs before and after POSS modification were observed by AFM (NT-MDT Co., Moscow, Russia). The morphologies of the fractured surface of CFs/MPSR composites were characterized by SEM (Quanta 200FEG, Hitachi Instrument, Inc. Japan).

Dynamic contact angle tests were carried out by using a dynamic contact angle meter and tensiometer (DCAT21, Data Physics Instruments, Germany). Deionised water ($\gamma^d = 21.8 \text{ mN} \cdot \text{m}^{-1}$, $\gamma = 72.8 \text{ mN} \cdot \text{m}^{-1}$) and diiodomethane ($\gamma^d = 50.8 \text{ mN} \cdot \text{m}^{-1}$, $\gamma = 50.8 \text{ mN} \cdot \text{m}^{-1}$, 99% purity, Alfa Aesar, USA) were used as the test liquids. The dispersive and polar components of the CFs can be easily calculated according to the following equation:

$$\gamma_1(1 + \cos \theta) = 2(\gamma_1^p \gamma_f^p)^{1/2} + 2(\gamma_1^d \gamma_f^d)^{1/2} \quad (1)$$

$$\gamma_f = \gamma_f^p + \gamma_f^d \quad (2)$$

where γ_l , γ_l^d and γ_l^p are the surface tension of the test liquid, its dispersive and polar component, respectively.

Single fiber tensile tests of CFs were carried out on a universal testing machine (5569, Instron, USA) according to ASTM D3379-75. A gauge length of 100 mm and cross-head speed of $10 \text{ mm}\cdot\text{min}^{-1}$ were used for all samples. The results were analyzed using Weibull statistical method.

The CFs/MPSR composites ILSS was tested on a universal testing machine (WD-1, Changchun, China) with a three-point short-beam bending test method based on ASTM D2344. Specimen dimensions were $20 \text{ mm} \times 6 \text{ mm} \times 2 \text{ mm}$. The specimens and an enclosed space in where the test was conducted were maintained at room temperature. The specimens were tested at a cross-head speed of $2 \text{ mm}\cdot\text{min}^{-1}$. The ILSS values were calculated from:

$$ILSS = \frac{3P_b}{4bh} \quad (3)$$

where P_b is the maximum compression load at fracture (N), b is the width of the specimen (mm), h is the thickness of the specimen (mm).

Impact tests were carried out on a drop weight impact test system (9250HV, Instron, USA). The specimen dimensions were $55 \text{ mm} \times 6 \text{ mm} \times 2 \text{ mm}$. The impact span is 40 mm. The drop weight was 3 kg and the velocity was $1 \text{ m}\cdot\text{s}^{-1}$.

The thermal oxidative aging experiments were performed to investigate the heat

oxidation resistant properties of composites. Specimen dimensions were 20 mm × 6 mm × 2 mm. The composites were air pyrolyzed in the muffle furnace under isothermal condition at three different temperatures (300, 350 and 400 °C) for 30 min. The composite ILSS was tested according to the foregoing method.

3. Results and discussion

3.1 Surface chemical elemental composition of CF

FTIR is a sensitive technique to analyze surface functional groups of CFs. Fig. 3 shows the FTIR spectra of untreated CF and CF-g-POSS. For untreated CF, in addition to the bonds of the adsorbed water on the fiber surface and carbon dioxide in the air, there are some organic groups that can be observed. The broad band in the range of 2800-2980 cm^{-1} is assigned to the stretching vibration of C-H of methyl and methylene groups, the bands centered at about 1050-1100 cm^{-1} and 1580-1699 cm^{-1} correspond to the stretching vibration of C-C and C=C, respectively.¹⁶ For CF-g-POSS, many new characteristic peaks are obviously detected. The peak at 1641 cm^{-1} corresponds to the C=O stretching of the amide functionality (amide I band), and the peak at 1550 cm^{-1} is assigned to the combination of the bending N-H vibration (amide II band) and the C-N stretching of amide.³⁹ The strong bands at 998 and 1105 cm^{-1} are assigned to the Si-OH and Si-O-Si stretching vibrations of POSS, respectively.⁴⁰ The bands at 1259 and 801 cm^{-1} are related to the bending and stretching vibrations of Si-C groups, respectively.³⁶ All these observations confirm that POSS has been successfully grafted onto the surface of CFs.

Insert Fig. 3 here

XPS was carried out to examine the surface chemical composition of CFs.⁴¹ The surface elemental composition of CFs before and after POSS grafting was detected by XPS and the results are summarized in Table 1. The surface of untreated CF was composed mainly of carbon, oxygen and a small amount of nitrogen elements. After being grafted with TDI, the content of carbon element decreased obviously from 81.61% to 72.95% and the content of oxygen element increased from 17.47% to 20.22%. In addition, the surface atomic O/C ratios increased from 0.21 to 0.28, and the nitrogen element with 6.83% was observed on the fiber surface, suggesting that the TDI was grafted on the surface of CFs successfully. For CF-g-POSS, noticeable silicon element with a content of 7.62% was detected and the surface atomic Si/C ratios significantly grew to 0.11. All the observations indicated that TriSilanolPhenyl-POSS nanoparticles were grafted successfully onto the fiber surface.

Insert Table 1 here

The C1s spectra were peak fitted to detect the surface functional groups of CFs and the grafting reaction mechanisms. Fig. 4 shows the XPS C1s curve fit spectra of untreated CF, CF-TDI and CF-g-POSS. The C1s peaks of untreated CF (Fig. 4a) were deconvoluted into five component peaks: sp^2 C=C bonding in the graphitic structure of CFs (284.5 eV), C-C bonding of amorphous carbon (285.2 eV), C-O bond (286.6 eV), C=O bond (287.8 eV) and COOH bond (288.9 eV).⁴² After interaction with TDI, the C1s high-resolution spectrum results (Fig. 4b) showed two additional binding energy

peaks at 287.8 eV and 285.8 eV, which are attributed to a new bond generated on the fiber surface (-NH-C=O) between hydroxyl groups of the fiber surface and isocyanate groups of TDI and the C-N bonds in molecular structure of TDI. It indicated that TDI was grafted chemically onto the surface of CFs. From the XPS C1s core-level spectrum of CF-g-POSS (Fig. 4c), the content of -NH-C=O increased sharply, which signified that the reserved isocyanate groups of CF-TDI have reacted with hydroxyl groups of TriSilanolPhenyl-POSS. In addition, the C-Si (283.6 eV) is observed originating from the introduction of TriSilanolPhenyl-POSS onto the fiber surface.

In short, through the analysis of FTIR and XPS results, we conclude that the surface of CFs have been grafted with TriSilanolPhenyl-POSS using bridging TDI.

Insert Fig. 4 here

3.2 Surface topography of CF

SEM and AFM images of untreated CF and CF-g-POSS are shown in Fig. 5. Significant differences of surface topography between untreated CF and CF-g-POSS are observed. As shown in Fig. 5a and c, the untreated CF shows a relatively smooth and neat surface with some narrow parallel grooves distributed along the longitudinal direction of fibers. After modification, the CF-g-POSS surface (Fig. 5b and d) becomes much rougher and a layer of POSS nanoparticles are scattered onto the fiber surface and the grooves uniformly. In addition, the surface roughness (R_a) of CF-g-POSS increases to 97.1 nm from 48.6 nm of untreated one. The increased R_a can provide more contact area and improve mechanical interlocking between CFs and MPSR matrix, and thus enhance the

interfacial strength of composites.

Insert Fig. 5 here

3.3 Dynamic contact angle analysis

It is well known that the properties of composites are closely related to the wettability between the fiber and matrix resin. The surface functionality and topography of CFs can change significantly the fiber surface free energy. The enhancement of the fiber surface energy could promote better wettability between CFs and matrix, and good wettability usually leads to a high interfacial performance. The advancing contact angle (θ), the surface energy (γ), its dispersion component (γ^d) and polar component (γ^p) of untreated CF and CF-g-POSS are given in Table 2. As presented in Table 2, the surface energy of untreated CF was $35.87 \text{ mN}\cdot\text{m}^{-1}$, with a dispersion component of $29.21 \text{ mN}\cdot\text{m}^{-1}$ and a polar component of $6.66 \text{ mN}\cdot\text{m}^{-1}$. After POSS grafting, the surface energy and its components of CF-g-POSS increased significantly in comparison with those of untreated CF. In addition, the contact angles decreased from 58.90° to 51.22° for non-polar diiodomethane and from 78.50° to 61.43° for polar water. The improved polar component could be interpreted by many hydroxyl groups supplied by TriSilanolPhenyl-POSS grafted onto the fiber surface. The improved dispersion component could be ascribed to the different chemical composition of the fiber surface and the increased fiber surface roughness caused by TriSilanolPhenyl-POSS grafting. The enhancement of surface energy can improve effectively the compatibility of fiber surface with matrix resin and lead to better interfacial properties.

Insert Table 2 here

3.4 Single fiber tensile testing

The effect of TriSilanolPhenyl-POSS grafting on the tensile strength (TS) of CFs is evaluated by single fiber tensile testing. The fiber tensile testing results of different CFs are shown in Fig. 6. The untreated CF had a TS of 3.354 GPa. After modification, the TS of CF-g-POSS decreased slightly to 3.351 GPa, which may originate from the unavoidable introduction of surface defects during oxidation and grafting treatment. However, the damage of TriSilanolPhenyl-POSS grafting procedures to CFs is not as serious as expected normally and the reduction can be neglected. The analysis of TS results implies that POSS functionalization would not result in any discernable decrease in in-plane performance of composites. TriSilanolPhenyl-POSS grafting method can maintain the TS at maximum extent and enhance interfacial strength significantly.

3.5 Interfacial property testing

The ILSS results for untreated CF and CF-g-POSS composites are showed in Fig. 6. From Fig. 6, it can be clearly observed that the introduction of TriSilanolPhenyl-POSS coupling agent improve greatly the interfacial strength of CFs/MPSR composites. The ILSS of CF-g-POSS composites is 41.82 MPa, with an increase of 41.91% compared with the untreated CF (29.47 MPa). The enhancement in the ILSS can be attributed mainly to an improvement in chemical bonding, fiber surface energy and mechanical interlocking between the fibers and MPSR matrix. Zhao et al.³⁷ have reported that the ILSS of CFs/epoxy composites was increased by 18.10% through surface grafting of

ctaglycidyl dimethylsilyl POSS on CFs. Jiang et al.⁴³ have reported that the ILSS of unsaturated polyester composites was increased by 22.90% by chemically grafting amino-POSS onto the surface of CFs using triethylphosphodichloride as the bridging agent. The enhancement of the percentages is lower than the observed ILSS value here with surface grafting of TriSilanolPhenyl-POSS onto CFs.

To further study the mechanism for such an enhancement, the cryo-fractured surface morphologies of composites were examined by SEM, as illustrated in Fig. 7. For untreated CFs/MPSR composites (Fig. 7a), a great many CFs were pulled out from the MPSR matrix, and some big holes remained in the matrix. The interface de-bonding was observed obviously, which indicated a poor interfacial adhesion between CFs and MPSR. After TriSilanolPhenyl-POSS functionalization (Fig. 7b), the pulled-out CFs decreased and the pullout length of fibers was very short. Moreover, there is almost no interface debonding, suggesting the improved interface between CFs and MPSR after modification. As mentioned above, TriSilanolPhenyl-POSS nanoparticles not only link to CFs by chemical interaction, but also react with silanol end groups of MPSR during the curing process. As a result, the improved interface between CFs and MPSR through strong chemical bonding is responsible for the improvement in the interfacial performance.

Insert Fig. 6 and 7 here

3.6 Impact property testing

The impact performance of composites is affected mainly by the interface region between CFs and MPSR matrix. Fig. 8 shows the impact property testing results of

composites reinforced with untreated CF and CF-g-POSS. The impact strength of the untreated CFs/MPSR composites was $58.46 \text{ kJ}\cdot\text{m}^{-2}$. After being grafted with POSS, the impact strength of composites increased sharply to $75.21 \text{ kJ}\cdot\text{m}^{-2}$ owing to the improvement of interface containing TriSilanolPhenyl-POSS as discussed above. The energy required to destroy the interface increased. The schematic illustration of the interface of composites is given in Fig. 8a and b. Without an appropriate interface, the crack tip extends perpendicularly to the surface of CFs, which can result in fiber fracture under a small load. Massive POSS nanoparticles grafted onto the fiber surface can induce more cracks to absorb fracture energy efficiently and increase the fracture area when the crack passed to them. The TriSilanolPhenyl-POSS interface serving as a shielding layer can lighten the stress concentration, prevent the crack tips from contacting the fiber surface directly and make the crack path deviate away from the fiber surface to the interface region.³⁵

Insert Fig. 8 here

3.7 Thermal oxidative aging property testing

POSS hybrid materials have superior thermal stability and usually work as ideal reinforcing fillers to improve the thermal properties of polymer matrix.⁴⁴⁻⁴⁶ The main purpose of thermal oxidative aging property testing is to evaluate the potential possibility of MPSR composites by grafting POSS that are used in high temperature aerospace applications. The ILSS results of composites reinforced with untreated CF and CF-g-POSS after thermal oxidation treatments are showed Fig. 9. From Fig. 9, it can be clearly seen that the ILSS of composites decreases with an increase in the

temperature for untreated CF and CF-g-POSS composites. However, the CF-g-POSS composites ILSS is much higher than that of untreated composites at the corresponding temperature. Based on the outstanding heat resistance of CFs and MPSR, both of composites after 300 °C treatment for 30 min decreased slightly in ILSS. After 350 °C treated, the composites ILSS increased from 26.91 MPa for untreated CF to 39.12 MPa for CF-g-POSS by 45.37%. After thermal pyrolysis at 400 °C for 30 min, the modification composites ILSS composites remained at 34.68 MPa, 48.97% higher than untreated composites at the corresponding temperature, which exceeded greatly the untreated composites ILSS (29.47 MPa) at room temperature. The enhancement of thermal oxidative aging performance can be attributed mainly to an improvement interfacial strength and the excellent heat resistance of TriSilanolPhenyl-POSS. Numerous POSS cages grafted onto CFs can serve as barriers to prevent effectively the diffusion of oxygen and hinder the mobility of molecular chains at high temperature, which could reduce the weakening of interphase between CFs and MPSR matrix. In addition, uniform POSS nanoparticles of the fiber surface can form an inorganic SiO₂ layer upon exposure to thermal oxidation treatments. The SiO₂ protective layer helps to protect effectively the interface and prevent the composites from further oxidative degradation.

Insert Fig. 9 here

4. Conclusions

TriSilanolPhenyl-POSS was grafted successfully onto the CF surface by bridging TDI and enhanced effectively the interfacial properties and thermo-oxidative stability of

CFs/MPSR composites. The polarity, wettability and surface roughness of CFs after TriSilanolPhenyl-POSS grafting increased obviously owing to the enhancement in reactive groups, surface free energy and roughness. The ILSS (41.82 MPa) and impact strength ($75.21 \text{ kJ}\cdot\text{m}^{-2}$) of CF-g-POSS/MPSR composites were dramatically increased compared with that of the CFs/MPSR composites (29.47 MPa and $58.46 \text{ kJ}\cdot\text{m}^{-2}$) resulting from strengthened interfacial adhesion. Moreover, an improved interfacial adhesion between CF-g-POSS and matrix resin could be confirmed from SEM observations of the cryo-fractured surfaces. Additionally, the thermal oxidation resistance of composites by grafting TriSilanolPhenyl-POSS was superior to that of untreated composites. Meanwhile, the TriSilanolPhenyl-POSS functionalization processes did not result in any discernable decrease in TS. We anticipate that this study will provide valuable guidance for fabricating multifunctional CFs reinforcements with simultaneously improved interfacial performance and heat oxidation resistance.

Acknowledgements

The authors gratefully acknowledge the National High Technology Research and Development Program of China (863 Program, grant number 2012AA03A212).

References

- 1 J. D. Jovanovic, M. N. Govedarica, P. R. Dvornic and I. G. Popovic, *Polym. Degrad. Stab.*, 1998, **61**, 87-93.
- 2 Y. Zhang, Y. Huang, X. Liu and Y. Yu, *J. Appl. Polym. Sci.*, 2003, **89**, 1702-1707.
- 3 H. Lord and S. O. Kelley, *J. Mater. Chem.*, 2009, **19**, 3127-3134.
- 4 M. C. Paiva, C. A. Bernardo and M. Nardin, *Carbon*, 2000, **38**, 1323-1337.

- 5 W.-H. Liao, H.-W. Tien, S.-T. Hsiao, S.-M. Li, Y.-S. Wang, Y.-L. Huang, S.-Y. Yang, C.-C. M. Ma and Y.-F. Wu, *ACS Appl. Mater. Inter.*, 2013, **5**, 3975-3982.
- 6 M. M. Hassan, L. Schiermeister and M. P. Staiger, *RSC Adv.*, 2015, **5**, 55353-55362.
- 7 C. Pradere, J. C. Batsale, J. M. Goyh  n  che, R. Pailler and S. Dilhaire, *Carbon*, 2009, **47**, 737-747.
- 8 X. Q. Zhang, X. Y. Fan, C. Yan, H. Z. Li, Y. D. Zhu, X. T. Li and L. P. Yu, *ACS Appl. Mater. Inter.*, 2012, **4**, 1543-1552.
- 9 X. Zhang, O. Alloul, Q. L. He, J. H. Zhu, M. J. Verde, Y. T. Li, S. Y. Wei and Z. H. Guo, *Polymer*, 2013, **54**, 3594-3604.
- 10 H. B. Gu, S. Tadakamalla, Y. D. Huang, H. A. Colorado, Z. P. Luo, N. Haldolaarachchige, D. P. Young, S. Y. Wei and Z. H. Guo, *ACS Appl. Mater. Inter.*, 2012, **4**, 5613-5624.
- 11 C. Zhang, J. Hankett and Z. Chen, *ACS Appl. Mater. Inter.*, 2012, **4**, 3730-3737.
- 12 Q. Y. Peng, Y. B. Li, X. D. He, H. Z. Lv, P. A. Hu, Y. Y. Shang, C. Wang, R. G. Wang, T. Sritharan and S. Y. Du, *Compos. Sci. Technol.*, 2013, **74**, 37-42.
- 13 Z. W. Xu, L. Chen, Y. D. Huang, J. L. Li, X. Q. Wu, X. M. Li and Y. N. Jiao, *Eur. Polym. J.*, 2008, **44**, 494-503.
- 14 I. D. Harry, B. Saha and I. W. Cumming, *Carbon*, 2007, **45**, 766-774.
- 15 M. A. Montes-Mor  n, A. Mart  nez-Alonso, J. M. D. Tasc  n, M. C. Paiva and C. A. Bernardo, *Carbon*, 2001, **39**, 1057-1068.
- 16 L. C. Ma, L. H. Meng, Y. W. Wang, G. S. Wu, D. P. Fang, Y. J. Li, M. W. Qi and Y. D. Huang, *RSC Adv.*, 2014, **4**, 39156-39166.

- 17 X. Q. Zhang, H. B. Xu and X. Y. Fan, *RSC Adv.*, 2014, **4**, 12198-12205.
- 18 L. M. Gao, T.-W, Chou, E. T. Thostenson and Z. G. Zhang, *Carbon*, 2010, **48**, 3788-3794.
- 19 W. Z. Qin, F. Vautard, P. Askeland, J. R. Yu and L. Drzal, *RSC Adv.*, 2015, **5**, 2457-2465.
- 20 Z. W. Xu, Y. D. Huang, C. H. Zhang, L. Liu, Y. H. Zhang and L. Wang, *Compos. Sci. Technol.*, 2007, **67**, 3261-3270.
- 21 H. B. Gu, S. Tadakamalla, X. Zhang, Y. D. Huang, Y. Jiang, H. A. Colorado, Z. P. Luo, S. Y. Wei and Z. H. Guo, *J. Mater. Chem. C*, 2013, **1**, 729-743.
- 22 Q. L. He, T. T. Yuan, X. R. Yan, D. W. Ding, Q. Wang, Z. P. Luo, T. D. Shen, S. Y. Wei, D. P. Cao and Z. H. Guo, *Macromol. Chem. Phys.*, 2014, **215**, 327-340.
- 23 Y.-J. Wan, L.-C. Tang, L.-X. Gong, D. Yan, Y.-B. Li, L.-B. Wu, J.-X. Jiang and G.-Q. Lai, *Carbon*, 2014, **69**, 467-480.
- 24 C. Vallés, I. A. Kinloch, R. J. Young, N. R. Wilson and J. P. Rourke, *Compos. Sci. Technol.*, 2013, **88**, 158-164.
- 25 J. H. Park and S. C. Jana, *Macromolecules*, 2003, **36**, 2758-2768.
- 26 J. H. Zhu, S. Y. Wei, A. Yadav and Z. H. Guo, *Polymer*, 2010, **51**, 2643-2651
- 27 L. L. Qu, L. J. Wang, X. M. Xie, G. Z. Yu and S. H. Bu, *RSC Adv.*, 2014, **4**, 64354-64363.
- 28 J. Guo, X. Zhang, H. B. Gu, Y. R. Wang, X. R. Yan, D. W. Ding, J. Long, S. Tadakamalla, Q. Wang and M. A. Khan, *RSC Adv.*, 2014, **4**, 36560-36572.
- 29 A. Lee, J. Xiao and F. J. Feher, *Macromolecules*, 2005, **38**, 438-444.

- 30 W. Q. Yu, J. F. Fu, X. Dong, L. Y. Chen and L. Y. Shi, *Compos. Sci. Technol.*, 2014, **92**, 112-119.
- 31 W. A. Zhang, B. Fang, A. Walther and A. H. E. Müller, *Macromolecules*, 2009, **42**, 2563-2569.
- 32 N. C. Escudé and E. Y.-X. Chen, *Chem. Mater.*, 2009, **21**, 5743-5753.
- 33 M. Sánchez-Soto, D. A. Schiraldi and S. Illescas, *Eur. Polym. J.*, 2009, **45**, 341-352.
- 34 W. C. Zhang, X. M. Li, X. Y. Guo and R. J. Yang, *Polym. Degrad. Stab.*, 2010, **95**, 2541-2546.
- 35 D. W. Jiang, L. X. Xing, L. Liu, X. R. Yan, J. Guo, X. Zhang, Q. B. Zhang, Z. J. Wu, F. Zhao and Y. D. Huang, *J. Mater. Chem. A*, 2014, **2**, 18293-18303.
- 36 F. Zhao and Y. D. Huang, *J. Mater. Chem.*, 2011, **21**, 3695-3703.
- 37 F. Zhao, Y. D. Huang, L. Liu, Y. P. Bai and L. W. Xu, *Carbon*, 2011, **49**, 2624-2632.
- 38 D. W. Jiang, L. X. Xing, L. Liu, S. F. Sun, Q. B. Zhang, Z. J. Wu, X. R. Yan, J. Guo, Y. D. Huang and Z. H Guo, *Compos. Sci. Technol.*, 2015, **117**, 168-175.
- 39 G.-X. Chen and H. Shimizu, *Polymer*, 2008, **49**, 943-951.
- 40 L. Kou and C. Gao, *Nanoscale*, 2011, **3**, 519-528.
- 41 G. X. Zhang, S. H. Sun, D. Q. Yang, J.-P. Dodelet and E. Sacher, *Carbon*, 2008, **46**, 196-205.
- 42 Y. X. Li, Y. B. Li, Y. J. Ding, Q. Y. Peng, C. Wang, R. G. Wang, T. Sritharan, X. D. He and S. Y. Du, *Compos. Sci. Technol.*, 2013, **85**, 36-42.
- 43 D. W. Jiang, L. Liu, J. Long, L. X. Xing, Y. D. Huang, Z. J. Wu, X. R. Yan and Z. H. Guo, *Compos. Sci. Technol.*, 2014, **100**, 158-165.
- 44 J.-c. Huang, C.-b. He, Y. Xiao, K. Y. Mya, J. Dai and Y. P. Siow, *Polymer*, 2003, **44**,

4491-4499.

45 Y. R. Liu, Y. D. Huang and L. Liu, *Polym. Degrad. Stab.*, 2006, **91**, 2731-2738.

46 A. Tsuchida, C. Bolln, F. G. Sernetz, H. Frey and R. Mülhaupt, *Macromolecules*, 1997, **30**, 2818-2824.

Figure captions

Fig. 1 The molecular structure of TriSilanolPhenyl-POSS.

Fig. 2 Schematic illustration of the functionalization procedure of CF-g-POSS.

Fig. 3 FTIR spectra of (a) untreated CF and (b) CF-g-POSS.

Fig. 4 XPS C1s high-resolution spectra of (a) untreated CF, (b) CF-TDI and (c) CF-g-POSS.

Fig. 5 SEM, AFM images of different CF surfaces: (a, c) untreated CF and (b, d) CF-g-POSS.

Fig. 6 TS of CFs and ILSS of CFs/MPSR composites.

Fig. 7 SEM morphologies of the fracture surface of composites reinforced with (a) untreated CF and (b) CF-g-POSS.

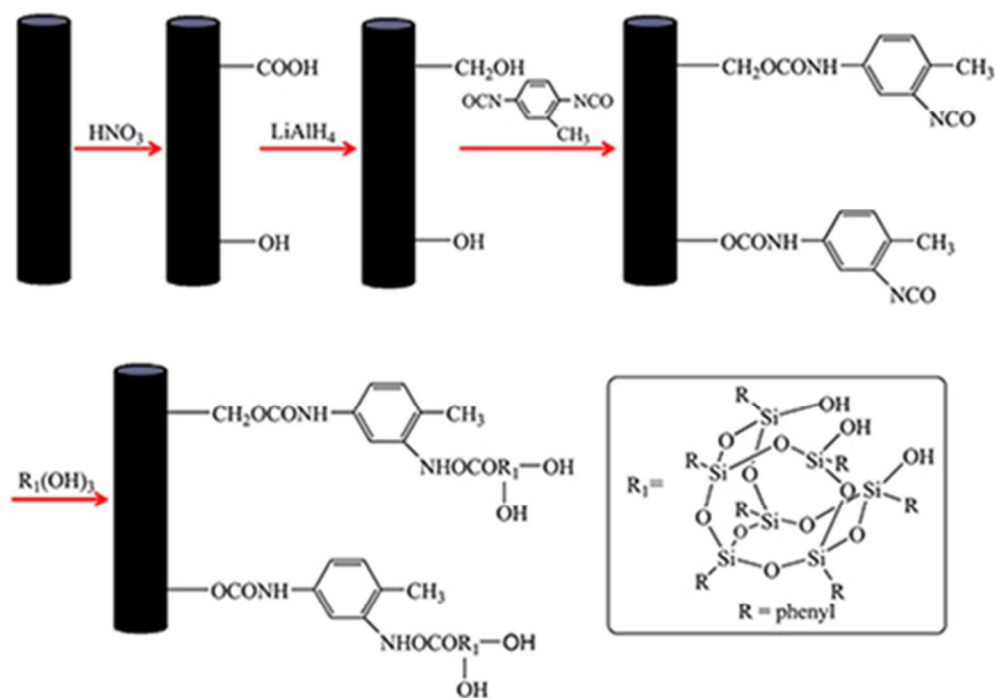
Fig. 8 Impact test results of composites and schematic of impact test of composites reinforced with (a) untreated CF and (b) CF-g-POSS.

Fig. 9 ILSS of CFs/MPSR composites after thermal oxidation treatments.

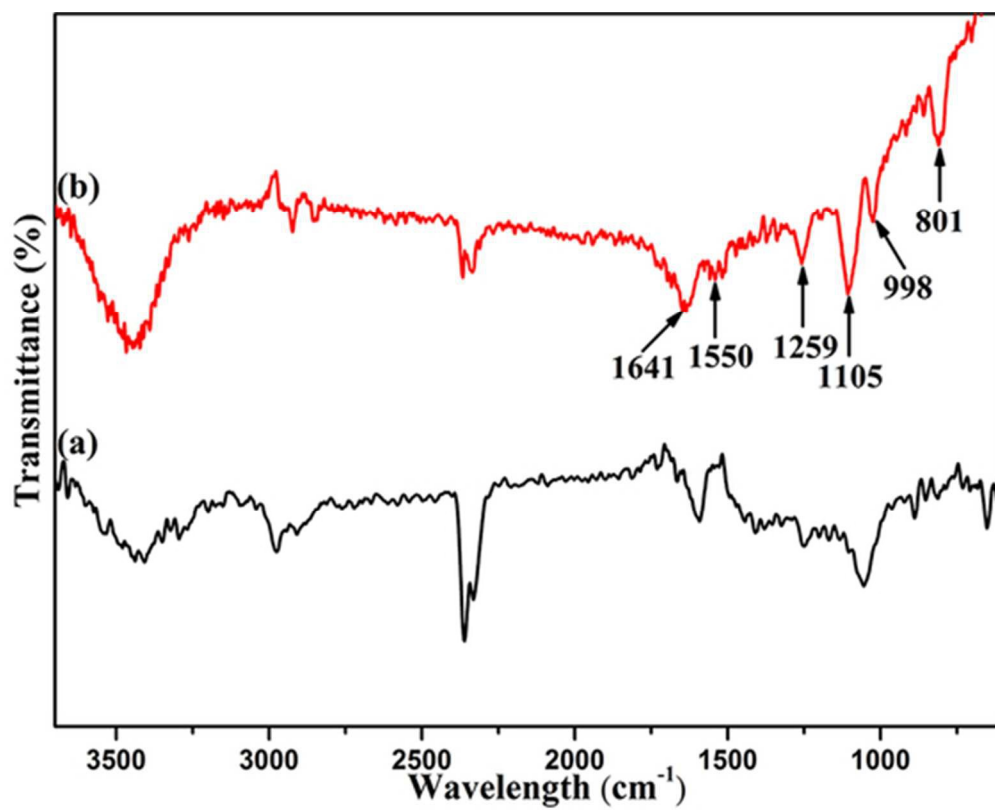
Table captions

Table 1 Surface element analysis of CFs.

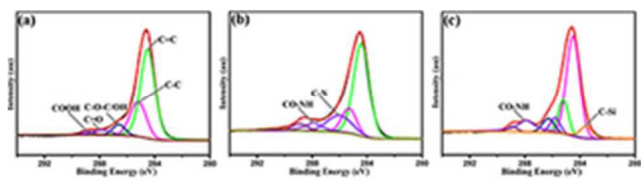
Table 2 Contact angles and surface energy of CFs.



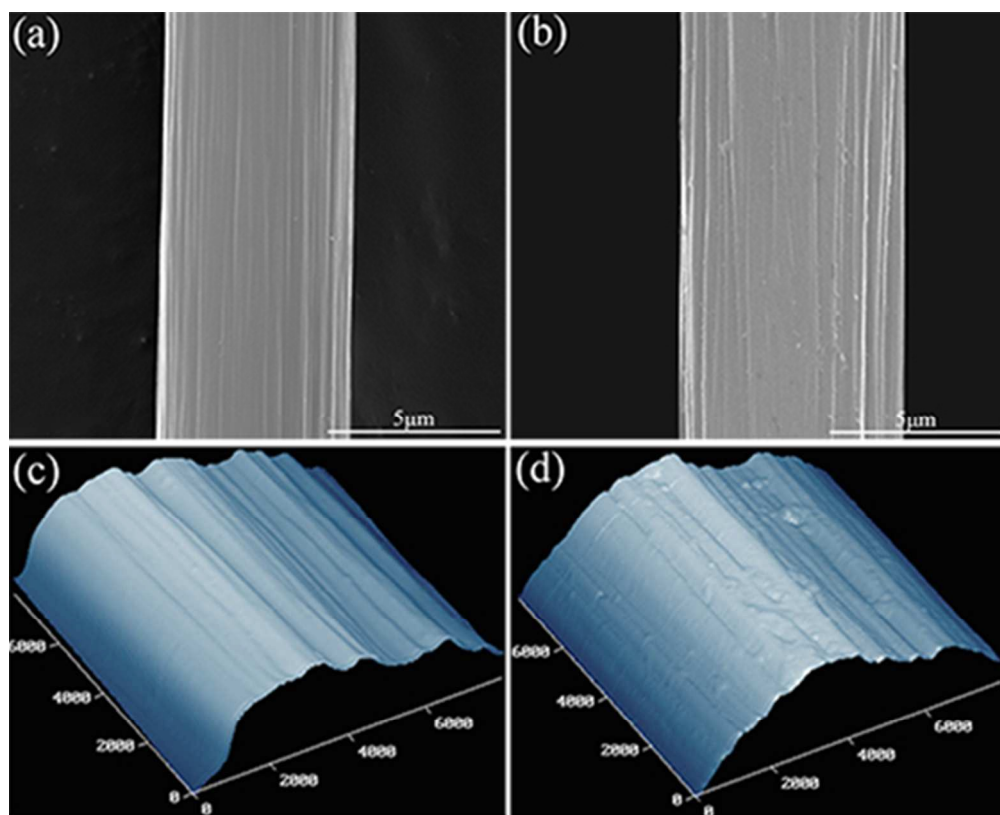
41x29mm (300 x 300 DPI)



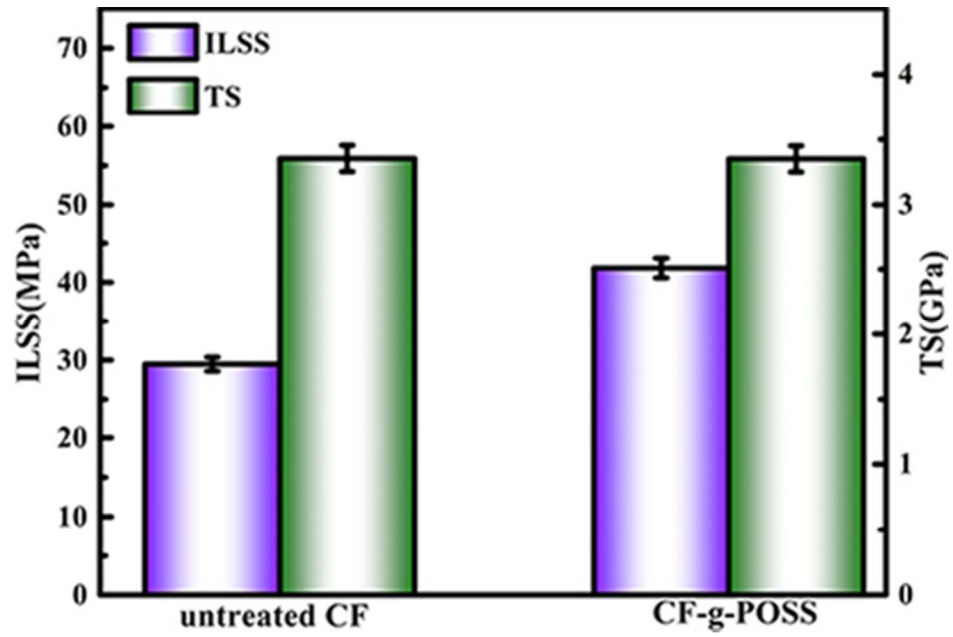
47x38mm (300 x 300 DPI)



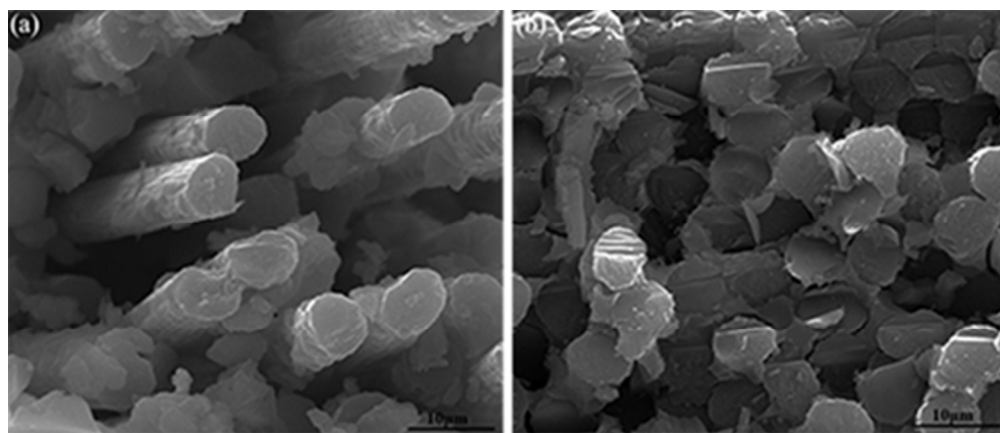
26x7mm (300 x 300 DPI)



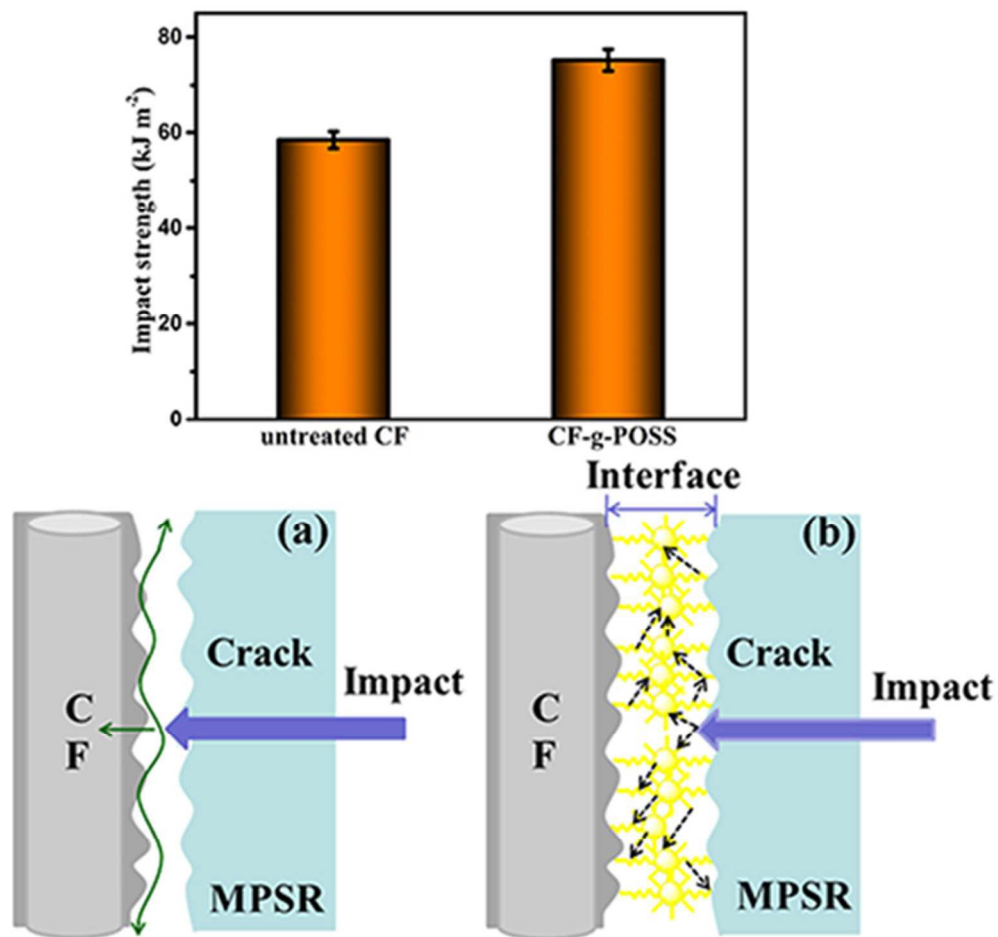
48x39mm (300 x 300 DPI)



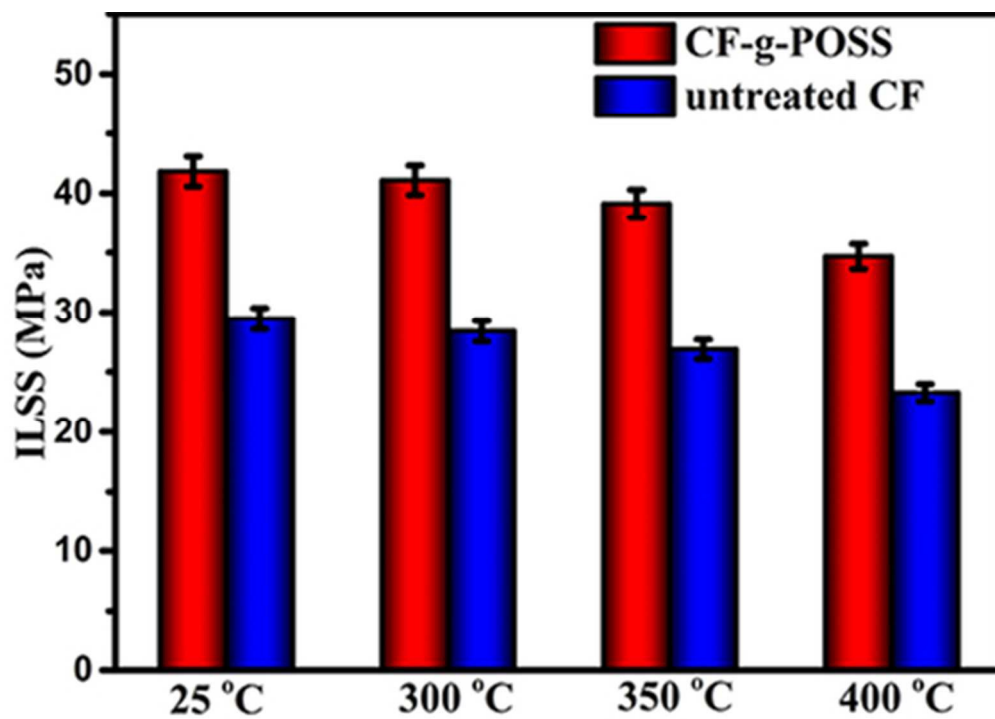
39x26mm (300 x 300 DPI)



42x18mm (300 x 300 DPI)



56x53mm (300 x 300 DPI)



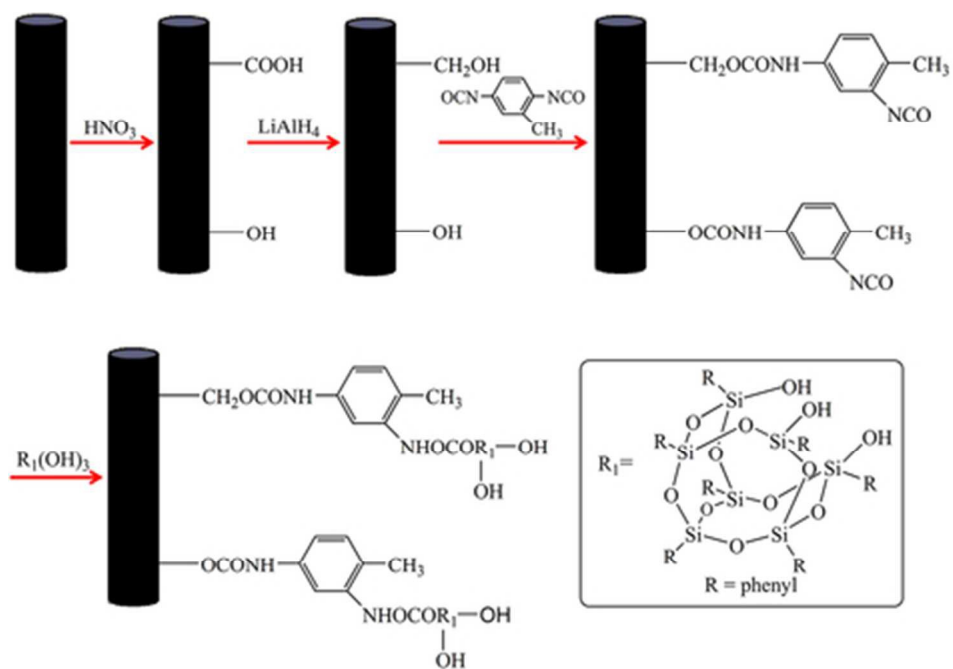
42x30mm (300 x 300 DPI)

Table 1 Surface element analysis of CFs

Samples	Element content (%)					
	C	N	O	Si	O/C	Si/C
Untreated CF	81.61	0.92	17.47	–	0.21	–
CF-TDI	72.95	6.83	20.22	–	0.28	–
CF-g-POSS	67.29	1.96	23.13	7.62	0.34	0.11

Table 2 Contact angles and surface energy of CFs

Samples	contact angles (°)		Surface energy (mN m ⁻¹)		
	θ_{water}	$\theta_{\text{diiodomethane}}$	γ^{d}	γ^{p}	γ
Untreated CF	78.50	58.90	29.21	6.66	35.87
CF-g-POSS	61.43	51.22	33.59	14.03	47.62



39x27mm (300 x 300 DPI)